Amino Acid Derivatives of Tungsten Carbonyl. Structure and Reactivity Investigations of Zerovalent Tungsten Glycine Derivatives

Donald J. Darensbourg,* Earl V. Atnip, Kevin K. Klausmeyer, and Joseph H. Reibenspies

Department of Chemistry, Texas A&M University, College Station, Texas 77843

Received May 26, 1994[⊗]

The amino acid derivatives of tungsten(0) $[Et_4N][W(CO)_4(O_2CCH_2NH_2)]$ (**1**), $[Et_4N][W(CO)_4(O_2CCH_2NHMe)]$ (**2**), and $[Et_4N][W(CO)_4(O_2CCH_2NMe_2)]$ (**3**) have been synthesized from the reaction of $W(CO)_5THF$ with the tetraethylammonium salt of the corresponding α-amino acid in a tetrahydrofuran solution. The glycine derivative, complex **1**, is highly soluble in water. The complexes have been characterized in solution by infrared and NMR spectroscopies and in the solid state by X-ray crystallography. Complex **1** crystallized in the orthorhombic space group $P2_12_12_1$ with $a = 10.408(14)$ Å, $b = 13.155(11)$ Å, $c = 13.657(10)$ Å, $V = 1870(3)$ Å^3, and $d_{calc} = 1.777$ g cm^{-3}, for $Z = 4$, from hexane/THF. Complex **2** crystallized in the monoclinic system, space group $P2_1/c$, with $a = 14.012(5)$ Å, $b = 10.335(2)$ Å, $c = 14.728(4)$ Å, $\beta = 112.28(2)°$, $V = 1973.5(8)$ Å^3, and $d_{calc} = 1.731$ g cm^{-3}, for $Z = 4$, from hexane/THF. Complex **3** crystallized in the triclinic space group $P\bar{1}$ with $a = 11.586(5)$ Å, $b = 11.711(6)$ Å, and $c = 15.068(7)$ Å, $\alpha = 90.01(4)°$, $\beta = 96.28(4)°$, $\gamma = 90.27(4)°$, $V = 2032(2)$ Å^3, and $d_{calc} = 1.727$ g cm^{-3}, for $Z = 4$, from a hexane-layered THF solution of **3**. The geometry of the anion in each case is that of a slightly distorted octahedral arrangement of four carbonyl ligands and a puckered five-membered glycinate chelate ring. Complexes **1** and **2** exihibit intermolecular hydrogen-bonding interactions with N···O distances of 2.746 and 2.826 Å, respectively. Weaker hydrogen-bonding interactions in solution with THF and CH_3CN are noted as well. Although the coordination environments about the tungsten centers of the three glycinate derivatives are essentially the same, the CO lability is greatly enhanced in complexes **1** and **2** as compared to complex **3**. This CO labilization in complexes **1** and **2** is attributed to a solvent-assisted removal of a proton from the amine ligand leading to a substitutionally labile amide transient species. Deprotonation of the amine ligand is aided by the π-donation of the thus formed amide ligand to the coordinatively unsaturated metal center in the reactive intermediate.

This study represents part of a systematic examination of the interactions and reactions of zerovalent group 6 metal carboxylates.[1] Specifically, we are interested in carboxylate ligands which possess additional functional groups for metal binding. These investigations are directed by a desire to better understand transition-metal catalyzed decarboxylation processes.[2] For example, we recently demonstrated that the electrophilic character of the metal center greatly influences the rate of C–C bond cleavage in the decarboxylation of the cyanoacetate ligand when bound *via* the cyano moiety.[3,4] The skeletal reaction is depicted in Scheme 1 for the decarboxylation of cyanoacetic acid catalyzed in the presence of $W(CO)_5O_2CCH_2CN^-$, where the site for acid binding is created by the labilizing ability of the bound carboxylate ligand.[5] Importantly, Cu(I), being a better electrophile than tungsten(0), is more effective at catalyzing the decarboxylation of cyanoacetic acid using both monomeric and dimeric Cu(I) catalyst precursors.

Scheme 1

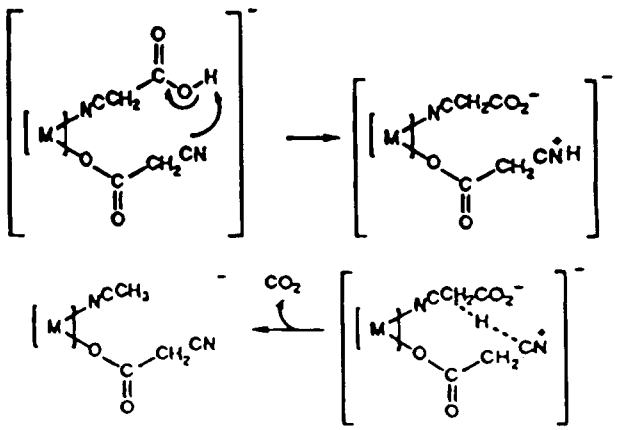

A logical and significant extension of these efforts would be analogous studies involving carboxylate ligands derived from amino acids. Indeed, the process of cleavage of the carbon–carbon bond in α-amino acids conforms to the requirement which facilitates the decarboxylation reaction, i.e., that the substrate has the ability to stabilize the developing carbanion transition state as the reaction proceeds to products (eq I). Some

[⊗] Abstract published in *Advance ACS Abstracts,* October 1, 1994.

(1) (a) Cotton, F. A.; Darensbourg, D. J.; Kolthammer, B. W. S. *J. Am. Chem. Soc.* **1981**, *103*, 398. (b) Darensbourg, D. J.; Rokicki, A. *J. Am. Chem. Soc.* **1982**, *104*, 349. (c) Cotton, F. A.; Darensbourg, D. J.; Kolthammer, B. W. S.; Kudaroski, R. *Inorg. Chem.* **1982**, *21*, 1656. (d) Darensbourg, D. J.; Kudaroski, R.; Bauch, C.G.; Pala, M.; Simmons, D.; White, J. N. *J. Am. Chem. Soc.* **1985**, *107*, 7463. (e) Tooley, P. A.; Ovalles, C.; Kao, S. C.; Darensbourg, D. J.; Darensbourg, M.Y. *J. Am. Chem. Soc.* **1986**, *108*, 5465. (f) Darensbourg, D. J.; Wiegreffe, H. P. *Inorg. Chem.* **1990**, *29*, 592. (g) Darensbourg, D. J.; Joyce, J. A.; Bischoff, C. J.; Reibenspies, J. H. *Inorg. Chem.* **1991**, *30*, 1137. (h) Darensbourg, D. J.; Joyce, J.A.; Rheingold, A. *Organometallics* **1991**, *10*, 3407. (i) Darensbourg, D. J.; Chojnacki, J. A.; Reibenspies, J. H. *Inorg. Chem.* **1992**, *31*, 3951.

(2) Deacon, G. B.; Faulks, S. J.; Pain, G. N. *Adv. Organomet. Chem.* **1986**, *25*, 237.

(3) Darensbourg, D. J.; Longridge, E. M.; Atnip, E. V.; Reibenspies, J. H. *Inorg. Chem.* **1992**, *31*, 3951.

(4) Darensbourg, D. J.; Longridge, E. M.; Holtcamp, M. W.; Klausmeyer, K. K.; Reibenspies, J. H. *J. Am. Chem. Soc.* **1993**, *115*, 8839.

(5) Darensbourg, D. J.; Chojnacki, J. A.; Atnip, E. V. *J. Am. Chem. Soc.* **1993**, *115*, 4675.

0020-1669/94/1333-5230$04.50/0

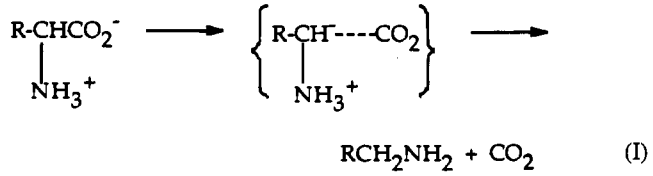

$$RCH_2NH_2 + CO_2 \qquad (I)$$

of the amines thus formed by these enzymatic reactions have important physiological effects. For example, Dopa decarboxylase decarboxylates 3,4-dihydroxyphenylalanine to form dopamine, a substance which is an intermediate in the formation of adrenaline.[6] The electron-releasing effect of NH_2CH_2 is greatly diminished upon protonization, as evidenced by the corresponding Taft σ^* parameter being much more positive in the latter instance, 0.50 *vs* 2.24.[7] Metal binding of the amine group is expected to have a similar electron-withdrawing effect. Although the literature is replete with examples of amino acid derivatives of transition metals in positive oxidation states,[8] zerovalent or low-valent transition metal derivatives of amino acids, in particular glycine, are extremely rare.[9] Most structurally characterized examples encompass complexes of Pt(II) and Ag(I).[10]

In this paper we describe the synthesis of a series of glycine derivatives of tungsten carbonyl. The structures of these derivatives have been fully delineated both in solution *via* infrared and $^{13}C/^{1}H$ NMR spectroscopies and in the solid state by X-ray crystallography. Furthermore, the reactivity of these derivatives toward carbon monoxide dissociation is examined as a function of the nature of the glycinate ligand.

Experimental Section

Methods and Materials. All manipulations were performed on a double-manifold Schlenk vacuum line under an atmosphere of argon or in an argon-filled glovebox. Solvents were dried and deoxygenated by distillation from the appropriate reagent under a nitrogen atmosphere. Photolysis experiments were performed using a mercury arc 450-W UV immersion lamp purchased from Ace Glass Co. Infrared spectra were recorded on a Mattson 6021 spectrometer with DTGS and MCT detectors. Routine infrared spectra were collected using a 0.10-mm CaF_2 cell. ^{13}C NMR spectra were obtained on a Varian XL-200 spectrometer. ^{13}CO was purchased from Cambridge Isotopes and used as received. $W(CO)_6$ was purchased from Strem Chemicals, Inc., and used without further purification. Microanalyses were performed by Galbraith Laboratories, Inc., Knoxville, TN.

Synthesis of [Et$_4$N][O$_2$CCH$_2$NRR′] Salts. The synthesis of $[Et_4N][O_2CCH_2NRR']$ was accomplished by the reaction of the corresponding α-amino acid, $NRR'CH_2COOH$ with one equivalent of Et_4NOH in methanol, where R = H or Me and R′ = H or Me. The mixture was stirred for 60 min, and the methanol was removed under vacuum, leaving a white solid product.

(6) Meister, A. *Biochemistry of the Amino Acids*, 2nd ed.; New York, Academic Press: 1965.

(7) (a) Taft, R. *J. Am. Chem. Soc.* **1952**, *74*, 3120. (b) Values taken from: *Lange's Handbook*, 12th ed.; Dean, J. A., Ed.; McGraw-Hill: New York, 1979.

(8) Laurie, S. H. In *Comprehensive Coordination Chemistry*; Wilkinson, G., Gillard, R. D., McCleverty, J. A., Eds.; Pergamon: Oxford, England, 1987; Vol. 2, Chapter 20.

(9) (a) Petri, W.; Beck, W. *Chem. Ber.* **1984**, *117*, 3265. (b) Meder, H.-J.; Beck, W. *Z. Naturforsch.* **1986**, *41B*, 1247. (c) Grotjahn, D. B.; Gray, T. L. *J. Am. Chem. Soc.* **1994**, *116*, 6969.

(10) (a) Baidima, I. A.; Podberezskaya, N. V.; Krylova, L. F.; Borisov, S. V.; Bakakin, V. V. *Zh. Strukt. Khim.* **1980**, *21*, 106. (b) Pozhidaev, A. I.; Simonov, M.A.; Kruglik, A. I.; Shestakova, N. A.; Mal'chikov, G. D. *Zh. Strukt. Khim.* **1975**, *16*, 1080. (c) Freeman, H. C.; Golomb, M. L. *Acta Crystallogr., Sect. B* **1969**, *25*, 1203. (d) Iakovidis, A.; Hadjiliadis, N.; Schollhorn, H.; Thewalt, U.; Trotscher, G. *Inorg. Chim. Acta* **1989**, *164*, 221. (e) Erickson, L.E.; Jones, G. S.; Blanchard, J.L.; Ahmed, K. J. *Inorg. Chem.* **1991**, *30*, 3147. (f) Aclard, C. B.; Freeman, H. C. *J. Chem. Soc. D.* **1971**, 1016. (g) Rao, J.K.M.; Viswamitra, M. A. *Acta Crystallogr., Sect. B* **1972**, *28*, 1484.

Table 1. Crystallographic Data for Complexes 1–3

	1	2	3
empirical formula	$C_{14}H_{24}N_2O_6W$	$C_{15}H_{26}N_2O_6W$	$C_{16}H_{28}N_2O_6W$
fw	500.20	514.2	528.25
space group	$P2_12_12_1$	$P2_1/c$	$P\bar{1}$
V, Å^3	1870(3)	1973.5(8)	2032(2)
Z	4	4	4
d_{calc}, g/cm^3	1.777	1.731	1.727
a, Å	10.408(14)	14.012(5)	11.586(5)
b, Å	13.155(11)	10.335(2)	11.711(6)
c, Å	13.657(10)	14.728(4)	15.068(7)
α, deg			90.01(4)
β, deg		112.28(2)	96.28(4)
γ, deg			90.27(4)
T, K	293.0	193	193
μ(Mo Kα), mm^{-1}	11.711 (Cu Kα)	6.007	5.715
wavelength, Å	1.541 78	0.710 73	0.710 73
R_F,[a] %	7.09	4.06	5.21
R_{wF},[a] %	18.73[b]	3.83	12.34[b]

[a] $R_F = \sum|F_o - F_c|/\sum F_o$ and $R_{wF} = \{[\sum w(F_o - F_c)^2]/(\sum wF_o^2)\}^{1/2}$. [b] $R_{wF} = \{[\sum w(F_o^2 - F_c^2)^2]/(\sum wF_o^2)\}^{1/2}$.

Synthesis of [Et$_4$N][W(CO)$_4$(O$_2$CCH$_2$NRR′)] Derivatives. The synthesis of $[Et_4N][W(CO)_4(O_2CCH_2NRR')]$ was accomplished on a 1.5 mmol scale in greater than 90% yield by the reaction of $W(CO)_5THF$ (prepared by photolysis of $W(CO)_6$ in THF) with 1 equiv of $[Et_4N][O_2CCH_2NRR']$ at ambient temperature, where R = H or Me and R′ = H or Me. The THF was removed from the reaction mixture by vacuum, and the remaining light yellow solid was washed with hexane three times to afford a bright yellow powder. Anal. Calcd for $[Et_4N][W(CO)_4(O_2CCH_2NH_2)]$ ($C_{14}H_{24}N_2O_6W$): C, 33.62; H, 4.84. Found: C, 32.83; H, 4.60. Anal. Calcd for $[Et_4N][W(CO)_4(O_2CCH_2NHMe)]$ ($C_{15}H_{26}N_2O_6W$): C, 35.04; H, 5.10. Found: C, 35.48; H, 5.51. Calcd for $[W(CO)_4(O_2CCH_2NMe_2)]$ ($C_{16}H_{28}N_2O_6W$): C, 36.38; H, 5.34. Found: C, 35.74; H, 5.49.

X-ray Crystallography of [Et$_4$N][W(CO)$_4$(O$_2$CCH$_2$NRR′)] Derivatives. Crystal data and details of data collection are given in Table 1. A light yellow-green needle crystal of **1** was mounted in a glass capillary at room temperature. A yellow parallelpiped crystal of **2** and an orange block crystal of **3** were mounted on a glass fiber with epoxy cement at room temperature and cooled to 193 K in a N_2 cold stream. Preliminary examination and data collection were performed on a Rigaku AFC5R X-ray diffractometer (Cu Kα, λ = 1.541 78 Å radiation) for **1** and a Nicolet R3m/v X-ray diffractometer (Mo Kα, λ = 0.710 73 Å radiation) for **2** and **3**. Cell parameters were calculated from the least-squares fitting of the setting angles for 24 reflections. ω scans for several intense reflections indicated acceptable crystal quality. Data were collected for $4.0° \le 2\theta \le 50.0°$. Three control reflections, collected every 97 reflections, showed no significant trends. Background measurements by stationary-crystal and stationary-counter techniques were taken at the beginning and end of each scan for half of the total scan time. Lorentz and polarization corrections were applied to 2186 reflections for **1**, 3852 for **2**, and 7452 for **3**. An empirical absorption correction was applied. A total of 2030 unique reflections for **1**, 2822 for **2**, and 4994 for **3**, with $|I| \ge 2.0\sigma(I)$, were used in further calculations. All three structures were solved by direct methods [SHELXS, SHELXTL-PLUS program package, Sheldrick (1988)]. Full-matrix least-squares anisotropic refinement for all non-hydrogen atoms yielded R = 0.071, R_w = 0.187, and S = 1.175 at convergence for **1**, R = 0.041, R_w = 0.038, and S = 2.86 for **2**, and R = 0.051, R_w = 0.123, and S = 1.018 for **3**. Hydrogen atoms were placed in idealized positions with isotropic thermal parameters fixed at 0.08. Neutral-atom scattering factors and anomalous scattering correction terms were taken from *International Tables for X-ray Crystallography*.

Kinetic Measurements. The rates of ^{13}CO exchange with complexes **1** and **2** were determined by placing an acetonitrile solution of the corresponding complex (0.10 mmol in 20 mL) under an atmosphere of ^{13}CO (>90% in ^{13}C). The solution was situated in a thermostated water bath at 40.0 °C (± 0.1°) and shaken periodically, and the exchange process was monitored by observing the decrease in absorbance of the highest frequency ν(CO) band of the starting complex as a function of time.

Table 2. Carbonyl Stretching Frequencies of $W(CO)_{4,5}(NRR'CH_2CO_2)^-$ Derivatives

complex[a]	ν(C≡O), cm^{-1}				ν(C=O), cm^{-1}	
					asym	sym
$W(CO)_5(NH_2CH_2CO_2)^-$	2066 (w)	1921 (vs)	1860 (m)[b,c]		1587	1457
$W(CO)_5(NHMeCH_2CO_2)^-$	2068 (w)	1923 (vs)	1868 (m)[b,c]			
$W(CO)_5(O_2CCH_2NHMe)^-$	2060 (w)	1910 (vs)	1852 (m)[c,d]		1640	
$W(CO)_5(O_2CCH_2NMe_2)^-$	2057 (w)	1908 (vs)	1852 (m)[c,d]		1642	1362
$W(CO)_4(O_2CCH_2NH_2)^-$	1996 (w)	1859 (vs)	1849 (sh)	1795 (m)[e]	1642	1367
$W(CO)_4(O_2CCH_2NHMe)^-$	1996 (w)	1859 (vs)	1847 (sh)	1798 (m)[e]	1638	1364
$W(CO)_4(O_2CCH_2NMe_2)^-$	1997 (w)	1859 (vs)	1846 (sh)	1801 (m)[e]	1644	

[a] As the tetraethylammonium salt. [b] Nitrogen-bound complex. [c] Spectra determined in THF. [d] Oxygen-bound complex. [e] Spectra determined in CH_3CN.

Table 3. ^{13}C NMR Data for the Carbonyl and Carboxylate Ligands in the $W(CO)_4(O_2CCH_2NRR')^-$ Anions[a]

complex[b]	^{13}C resonance, ppm[c]			
	CO(axial)	CO(trans to N)	CO(trans to O)	CO_2^-
$W(CO)_4(O_2CCH_2NH_2)^-$	205.5	216.0	216.8	180.5
$W(CO)_4(O_2CCH_2NHMe)^-$	205.3, 206.4	216.6	216.8	179.1
$W(CO)_4(O_2CCH_2NMe_2)^-$	206.3	216.9	217.0	177.9

[a] Spectra determined in acetonitrile-d_3. [b] As the tetraethylammonium salt. [c] The assignments of the ^{13}C signals for CO groups trans to N *vs* those trans to O are based on the general observation that the ^{13}C resonance for a CO group trans to N is upfield relative to a CO group trans to O in $W(CO)_5L$ derivatives. (See e.g.: Todd, L. J.; Wilkinson, J. R. *J. Organomet. Chem.* **1974**, *77*, 1. Reference 1f.) Nevertheless, in this instance the signals are quite close in value and an absolute distinction is not necessary at this time.

Scheme 2

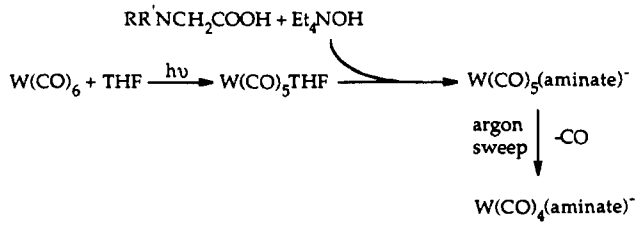

A similar kinetic run involving complex **1** was carried out exactly as described above in the presence of 50 μL of distilled, deionized, degassed H_2O. The rate of CO ligand exchange was only slightly enhanced in this instance (<25%).

The ^{13}CO exchange reaction was observed by ^{13}C NMR at high pressure of CO (700 psi) by noting the increase in signals due to the ^{13}C-labeled derivatives. Although we did not determine a rate constant for CO exchange by this technique, the rate of CO exchange was qualitatively similar to that determined by ν(CO) infrared spectroscopy.

Reaction of 1 with D_2O. A 50 mg (0.10 mmol) sample of $[Et_4N][W(CO)_4O_2CCH_2NH_2]$ was dissolved in 5 mL of CH_3CN. To this solution was added 50 μL (2.8 mmol) of D_2O. The solution was allowed to stir at room temperature for 2 days. The solvent was removed under vacuum, and the residue was redissolved with 5 mL of CH_3CN. The resulting solution gave infrared peaks assignable to ν(N−D) stretching modes at 2290 and 2245 cm^{-1}. The solvent was again removed under vacuum, and a solid state KBr infrared spectrum was obtained, providing ν(N−D) of 2290 and 2083 cm^{-1}.

Results

Synthesis. Complexes **1**−**3** were prepared in greater than 90% yield by the labile ligand displacement reaction of $W(CO)_5THF$ with the tetraethylammonium salt of the corresponding α-amino acid in tetrahydrofuran solution. The general approach to the synthesis of these complexes is outlined in Scheme 2. Complex **1** is highly water soluble, whereas complexes **2** and **3** are more sparingly soluble in water. Although the tetraethylammonium salts of glycine and sarcosine are only partially soluble in THF, these salts are rapidly drawn into solution as the substitution reaction occurs. In both these instances there was *in situ* solution infrared spectral evidence for initial formation of the tungsten pentacarbonyl amine derivatives prior to production of the final chelated product. That is, the initally formed tungsten pentacarbonyl species had ν(CO) bands in the frequency range anticipated for the amine bound derivative as opposed to the carboxylate bound derivative.[1i,11] Furthermore, evidence for the free carboxylate anion in the amine bound species is seen from the separation of the asym/sym $\nu(CO_2^-)$ bands of 130 cm^{-1}, whereas for the monodentate carboxylate-bonded species the corresponding separation is 280 cm^{-1}, as is expected.[12] However, because of the heterogeneity of this reaction mixture, it is unclear whether this preference of $W(CO)_5THF$ for the amine functionality of the anion is an inherent property of the amino carboxylate anion or an artifact of the reaction medium. Nevertheless, in the case of the tetrahydrofuran-soluble $Me_2NCH_2CO_2^-$ salt, the metal pentacarbonyl carboxylate bound *via* oxygen is the only observed intermediate prior to chelation. The reaction period for ring closure of 1.5−2.0 h at ambient temperature, carried out in an argon stream to impede CO recombination, is consistent with that expected on the basis of the LFER between the rate constant (k_1) for CO loss in $W(CO)_5O_2CR^-$ derivatives and the σ^* value for R.[1g] That is, the rate constant for CO loss in $W(CO)_5O_2CCH_2NH_2^-$ is predicted to be about 2.8×10^{-3} s^{-1} at 40 °C (σ^* for $-CH_2NH_2 = 0.50$).

Table 2 lists the infrared data for the ν(CO) region observed for the various reaction intermediates or products. As indicated in Table 2, the three amino acid tetracarbonyl derivatives have nearly identical ν(CO) band positions and intensity patterns. The electronic similarities of these derivatives is further illustrated by the ^{13}C NMR data compiled in Table 3. Data for the $-W(CO)_4$ moieties reveal a slight electronic difference in the equatorial CO ligands *trans* to oxygen versus nitrogen. Furthermore, for complex **2**, which possesses an unsymmetrically substituted amino group (i.e., the sarcosine derivative), the axial CO ligands are inequivalent. The coincidences in the electronic environment of the carboxylate carbon atoms are apparent as well in Tables 2 and 3, where the ν(C=O) vibrational modes and their ^{13}C resonances are listed respectively.

The glycine complex $W(CO)_4(O_2CCH_2NH_2)^-$ (**1**) in CH_3-

(11) Dennenberg, R. J.; Darensbourg, D. J. *Inorg. Chem.* **1972**, *11*, 72.
(12) Nakamoto, K. *Infrared and Raman Spectra of Inorganic and Coordination Compounds*, 4th ed.; Wiley: New York, 1986; p 231.

Table 4. Atomic Coordinates ($\times 10^4$) and Equivalent Isotropic Displacement Parameters ($Å^2 \times 10^3$) for $[Et_4N][W(CO)_4(O_2CCH_2NH_2)]$ (**1**)[a]

	x	*y*	*z*	*U*(eq)[b]
W1	2279(1)	−403(1)	−686(1)	58(1)
O1	4929(23)	−126(26)	−476(20)	127(2)
O2	3238(23)	−2085(12)	−2204(11)	72(16)
O3	2206(37)	1487(12)	736(15)	137(33)
O4	2131(26)	1093(11)	−2446(12)	83(19)
O5	228(19)	−631(14)	−642(15)	84(12)
O6	−1436(24)	−1743(17)	−139(20)	99(15)
N1	1948(30)	−1650(18)	497(16)	82(17)
N2	2490(35)	4439(20)	−1832(22)	107(14)
C1	3825(24)	−66(18)	−567(21)	66(2)
C2	2789(34)	−1530(16)	−1647(17)	60(19)
C3	2008(54)	939(17)	187(19)	132(40)
C4	2253(39)	551(15)	−1788(14)	75(23)
C5	723(33)	−2174(22)	354(20)	76(16)
C6	−212(37)	−1485(23)	−155(22)	76(14)
C7	1875(45)	5390(29)	−1685(33)	118(19)
C8	1333(45)	5910(25)	−2637(31)	119(27)
C9	2769(42)	4129(24)	−798(27)	109(19)
C10	3571(41)	3180(22)	−698(31)	114(27)
C11	1619(43)	3653(26)	−2247(28)	105(16)
C12	425(43)	3368(31)	−1694(32)	121(16)
C13	3667(43)	4448(32)	−2431(30)	115(16)
C14	4587(45)	5253(30)	−1999(32)	121(15)

[a] Estimated standard deviations are given in parentheses. [b] Equivalent isotropic *U* defined as one-third of the trace of the orthogonalized U_{ij} tensor.

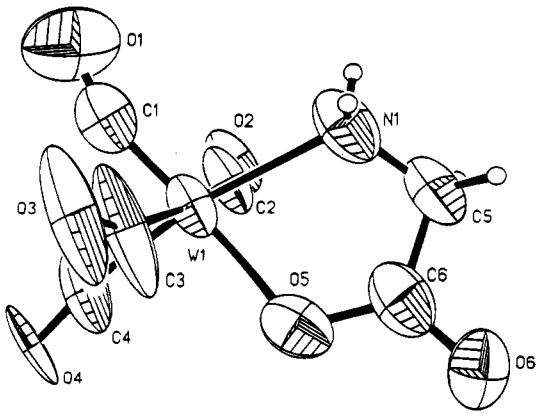

Figure 1. ORTEP diagram of the anion of complex **1**, showing 50% probability thermal motion ellipsoids with atomic numbering scheme.

CN exhibits two ν(N−H) stretching modes, free and hydrogen-bonded with solvent at 3349 and 3300 cm^{-1}, respectively. This is also observed in the solid-state infrared spectrum of **1**, where the free and hydrogen-bonded modes are found at 3344 and 3153 cm^{-1}. However, it is important to note that in solution the shift upon hydrogen bonding, $\Delta\nu$(N−D), is 49 cm^{-1} as compared to 191 cm^{-1} in the solid state. Indeed, the solid-state structure of complex **1** as determined by X-ray crystallography displays an extensive intermolecular hydrogen-bonding network (*vide infra*). These ν(N−D) vibrational modes shift to 2290 and 2245 cm^{-1} in acetonitrile solution and 2290 and 2083 cm^{-1} in KBr upon deuteration.

Structures. Crystals of complex **1** suitable for a single-crystal X-ray structure determination were grown by the slow diffusion of hexane into a concentrated THF solution of the complex over a 10 day period. Of particular interest was the crystals' habit; that is, the crystals were long fibers up to 1.5 in. in length. The final atomic positional and equivalent isotropic displacement parameters for complex **1** are listed in Table 4. Figure 1 shows a drawing of the anion, and selected bond distances and angles are provided in Table 5. The structure

Table 5. Selected Bond Lengths (Å) and Angles (deg) for $[Et_4N][W(CO)_4(O_2CCH_2NH_2)]$ (**1**)[a]

W1−C1	1.68(3)	W1−C4	1.96(2)
W1−C3	2.04(2)	W1−C2	2.05(2)
W1−O5	2.16(2)	W1−N1	2.33(2)
O1−C1	1.16(2)	O2−C2	1.15(2)
O3−C3	1.15(2)	O4−C4	1.15(2)
O5−C6	1.38(4)	O6−C6	1.32(4)
N1−C5	1.46(4)	C6−C6	1.50(4)
C1−W1−C4	85(2)	C1−W1−C3	82(2)
C4−W1−C3	86.2(11)	C1−C1−C2	90.3(13)
C4−W1−C2	88.6(9)	C3−W1−C2	171(2)
C1−W1−O5	169.7(10)	C4−W1−O5	95.6(13)
C3−W1−O5	88(2)	C2−W1−O5	100.0(11)
C1−W1−N1	105.1(12)	C4−W1−N1	169.2(14)
C3−W1−N1	97.9(10)	C2−W1−N1	88.4(9)
O5−W1−N1	74.7(9)	C6−O5−W1	117(2)
C5−N1−W1	112(2)	O1−C1−W1	161(3)
O2−C2−W1	170(3)	O3−C3−W1	161(5)
O4−C4−W1	174(4)	N1−C5−C6	110(3)
O6−C6−O5	122(3)	O6−C6−C5	118(3)
O5−C6−C5	120(3)		

[a] Estimated standard deviations are given in parentheses.

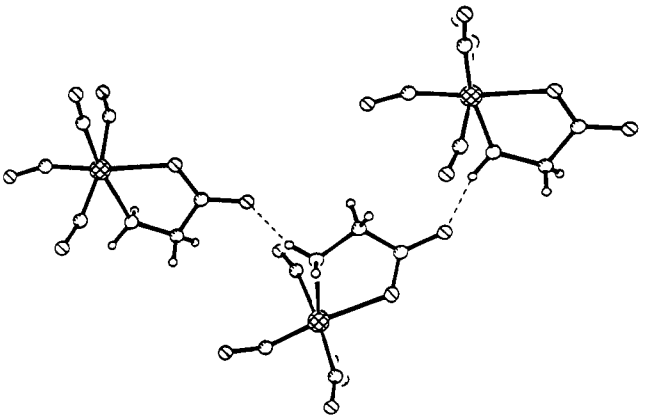

Figure 2. Ball and stick representation of the anion of complex **1** illustrating the intermolecular hydrogen bonding which forms helical chains.

of complex **1** consists of a glycinate residue which forms a chelate ring at the metal tetracarbonyl center through its nitrogen atom and one of its oxygen atoms to give a distorted octahedral coordination. The W−O bond distance of 2.156(21) Å is similar to that noted in other monodentate-bound carboxylates of tungsten; e.g., in $W(CO)_5O_2CCH_2CN^-$ and $W(CO)_5O_2CCH_3^-$ the W−O bond lengths are 2.220(3) Å and 2.207(4) Å, respectively.[1g,c] The W−N bond length was determined to be 2.328(22) Å, with the glycinate ligand forming a bite angle of 74.7(9)° with the metal atom.

As might be anticipated on the basis of the solid-state structure of glycine, the $W(CO)_4(O_2CCH_2NH_2)^-$ complex exhibits strong intermolecular N−H···O bonds formed between the N−H group and the distal oxygen of the carboxylate function on the adjacent metal complex. Interestingly, however, the hydrogen bonding which holds the complexes together is in the form of single helical infinite chains. This helix contains three metal anions per turn (Figure 2). Free glycine crystallizes in three distinct forms, α, β, and γ; each of which displays extensive intermolecular hydrogen bonding. The unstable β form exhibits hydrogen bonding which forms parallel planar sheets with no cross-sheet hydrogen bonding.[13] The α form is much the same except that it forms a pair of parallel planar sheets which are

(13) Iitaka, Y. *Acta Crystallogr.* **1960**, *13*, 35.

Table 6. Selected Internal Bond Distances (Å) in Free and Bound Glycine[a]

glycine form	N−C1	C1−C2	C2−O1	C2−O2
W-glycinate	1.43(40)	1.500(42)	1.319(42)	1.384(35)
α	1.474(5)	1.523(5)	1.252(5)	1.255(5)
β	1.484(15)	1.521(15)	1.233(15)	1.257(15)
γ	1.491(11)	1.527(11)	1.237(11)	1.254(11)

[a] Estimated standard deviations are given in parentheses. Atom-numbering scheme:

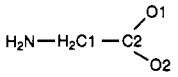

Table 7. Hydrogen-Bonding Distances (Å) in Free and Bound Glycine

glycine form	N···O	ref	glycine form	N···O	ref
W-glycinate	2.746	this work	β	2.758	13
α	2.768	14, 15	γ	2.687	16

linked together by cross-sheet hydrogen bonding.[14,15] The third, γ, form configures into infinite helical chains packed together with lateral hydrogen bonding between chains forming a three-dimensional network of hydrogen bonds.[16] This γ form of glycine is strongly piezoelectric along the axis of the helical chains. A comparison of bond lengths of the three forms of glycine and the metal-bound glycinate is provided in Table 6 with the atom-numbering scheme indicated. A comparison of some of the N···O distances in these various forms of glycine is given in Table 7; e.g., the N···O distance in complex **1** is 2.746 Å as compared to that of 2.768 Å seen in the ordinary α form of glycine.

In a manner analogous to that employed for complex **1**, single crystals of $[Et_4N][W(CO)_4(O_2CCH_2NHMe)]$ (**2**) and $[Et_4N][W(CO)_4(O_2CCH_2NMe_2)]$ (**3**) were obtained by the slow diffusion of hexane into a concentrated THF solution of the respective complex. The sarcosine derivative, **2**, crystallized, forming a polymeric structure similar to that of complex **1**, where the metal complex anions are linked by hydrogen bonding interactions, albeit somewhat weaker with a N···O distance of 2.826 Å. The final atomic positional and equivalent isotropic displacement parameters for complex **2** are listed in Table 8, with selected interatomic distances and angles provided in Table 9. Figure 3 illustrates the perspective drawing of the anion of complex **2** with the atomic numbering scheme. The structure of complex **2** is completely analogous to that of **1** with W−O and W−N distances of 2.203(5) and 2.299(8) Å with a glycinate bite angle of 73.4(2)°. The W−C distances are better defined in this structure as compared with the corresponding values in **1** with average $W-C_{ax} = 2.025[7]$ Å being slightly longer than the $W-C_{eq}$ bonds, which average 1.962[9] Å. However, there is not a significantly greater trans shortening of W−C bonds for W−CO groups trans to O *vs* N (1.947(8) vs 1.976(9) Å).

Unlike crystals of complex **1**, where the metal-bound glycinate ligand can participate in intermolecular hydrogen-bond formation, crystals of the tetraethylammonium salt of the dimethylamino carboxylate tungsten tetracarbonyl **3** were obtained as large blocks as opposed to long needles. The complex crystallized in the $P\bar{1}$ space group with two independent cations and two independent anions in the unit cell. Only slight differences in interatomic bond distances and angles are seen in the two distinct anions. The final atomic positional and equivalent isotropic displacement parameters are listed in Table 10, whereas all pertinent bond distances and angles in the anion are provided in Table 11. The $W(CO)_4(O_2CCH_2NMe_2)^-$ complex exists as a distorted octahedron (Figure 4), where the average O−C−W bond angle for the two carbonyl ligands in the axial positions is 168.9[10]°. The W−N and W−O bond lengths of 2.310(10) Å and 2.188(8) Å, respectively, are similar to those observed in complexes **1** and **2**. The carboxylate group of the bound *N,N*-dimethylglycinate ligand exhibits a moderate trans influence, as does the amine, with W−C bond lengths trans to these groups of 1.933(11) and 1.883(12) Å, respectively, compared to the average axial W−C bond length of 2.021[12] Å. The aminate ligand exhibits a bite angle of 73.6(3)° with the metal.

Table 8. Atomic Coordinates (×10⁴) and Equivalent Isotropic Displacement Parameters (Å² × 10³) for $[Et_4N][W(CO)_4(O_2CCH_2NHMe)]$ (**2**)[a]

	x	*y*	*z*	*U*(eq)[b]
W1	2715(1)	2012(1)	2295(1)	31(1)
O1	3368(4)	3940(5)	2805(4)	43(2)
O2	4665(5)	5300(6)	3056(5)	72(3)
O3	4197(5)	250(7)	4001(4)	69(3)
O4	745(5)	3009(7)	507(4)	66(3)
O5	1239(4)	1886(6)	3442(4)	51(3)
O6	1966(5)	−731(6)	1438(4)	64(3)
N1	3939(5)	2380(6)	1638(5)	34(3)
N2	1939(5)	6672(6)	3776(5)	38(3)
C1	4229(6)	4266(9)	2759(6)	49(4)
C2	4718(6)	3265(8)	2310(7)	48(4)
C3	3729(6)	978(8)	3410(6)	43(3)
C4	1502(6)	2726(8)	1146(6)	43(4)
C5	1781(6)	1957(6)	3018(5)	22(2)
C6	2234(7)	306(8)	1753(6)	43(3)
C7	3549(7)	2853(9)	618(6)	61(4)
C8	3062(6)	6806(9)	3887(7)	54(4)
C9	3842(8)	6593(12)	4915(8)	100(6)
C10	1681(8)	7557(8)	4458(7)	54(4)
C11	1926(10)	8973(10)	4404(9)	91(7)
C12	1742(6)	5279(7)	3995(6)	42(3)
C13	637(7)	4985(9)	3815(8)	72(5)
C14	1266(7)	7041(9)	2712(6)	55(4)
C15	1363(9)	6161(11)	1938(7)	87(5)

[a] Estimated standard deviations are given in parentheses. [b] Equivalent isotropic *U* defined as one-third of the trace of the orthogonalized U_{ij} tensor.

Table 9. Selected Bond Lengths (Å) and Angles (deg) for $[Et_4N][W(CO)_4(O_2CCH_2NHMe)]$ (**2**)[a]

W1−O1	2.203(5)	W1−N1	2.299(8)
W1−C3	2.022(7)	W1−C4	2.028(7)
W1−C5	1.976(9)	W1−C6	1.947(8)
O1−C1	1.28(1)	O2−C1	1.23(1)
O3−C3	1.15(1)	O4−C4	1.157(9)
O5−C5	1.15(1)	O6−C6	1.17(1)
N1−C2	1.479(9)	N1−C7	1.47(1)
		C1−C2	1.52(1)
O1−W1−N1	73.4(2)	O1−W1−C3	97.3(3)
N1−W1−C3	91.3(3)	O1−W1−C4	93.7(3)
N1−W1−C4	96.4(3)	C3−W1−C4	168.0(3)
O1−W1−C5	96.7(3)	N1−W1−C5	169.7(2)
C3−W1−C5	87.2(3)	C4−W1−C5	86.8(3)
O1−W1−C6	173.4(4)	N1−W1−C6	100.1(3)
C3−W1−C6	83.2(3)	C4−W1−C6	86.4(3)
C5−W1−C6	89.9(4)	W1−O1−C1	119.9(6)
W1−N1−C2	107.4(6)	W1−N1−C7	115.8(5)
C2−N1−C7	111.8(7)	O1−C1−O2	124.2(9)
O1−C1−C2	115.6(7)	O2−C1−C2	120.1(9)
N1−C2−C1	111.8(7)	W1−C3−O3	169.9(7)
W1−C4−O4	171.9(8)	W1−C5−O5	178.0(6)
W1−C6−O6	178.5(7)		

[a] Estimated standard deviations are given in parentheses.

(14) Marsh, R. E. *Acta Crstallogr.*. **1958**, *11*, 654.
(15) Power, L. F.; Turner, K. E.; Moore, F. H. *Acta Crystallogr., Sect. B* **1976**, *11*, 32.
(16) Iitaka, Y. *Acta Crystallogr.* **1961**, *14*, 1.

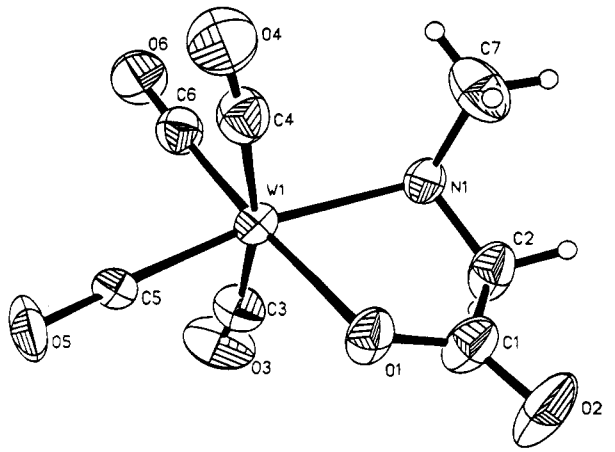

Figure 3. ORTEP diagram of the anion of complex **2**, showing 50% probability thermal motion ellipsoids with atomic numbering scheme.

Reactivity. As described in the previous sections the three glycine derivatives of tungsten carbonyl are structurally and electronically quite similar with respect to metal−ligand bonding. However, their reactivities in solution with regard to CO lability are noticeably different. That is, complex **1** readily loses a CO ligand at ambient temperature in CH_3CN or THF with concomitant formation of a tricarbonyl species (eq 1). For example, when argon is bubbled through an acetonitrile solution of **1**, in addition to the four bands listed in Table 2, new bands appear at 1885(s) and 1741(vs) cm^{-1} of the appropriate intensity ratio expected for a $-W(CO)_3$ moiety. Consistent with the structure depicted in eq 1, the ^{13}C NMR spectrum of the tricarbonyl derivative in CD_3CN at ambient temperature displayed three resonances due to carbonyl carbon atoms at 228.0, 226.1, and 225.1 ppm of approximately equal intensities. Furthermore, for a reaction mixture in CH_3CN consisting mostly of the tricarbonyl derivative, the $\nu(CO_2^-)$ bands were observed at 1636 and 1377 cm^{-1}, indicative of a monodentate bound carboxylate ligand. It is assumed that the tungsten tricarbonyl glycine anion contains a solvent molecule (CH_3CN or THF) in the metal's coordination sphere. Although there is ample precedent for well-characterized, coordinatively unsaturated group 6 metal carbonyl derivatives in the literature, in each of these instances strongly π-donating ligands such as aryloxides or arenethiolates are present.

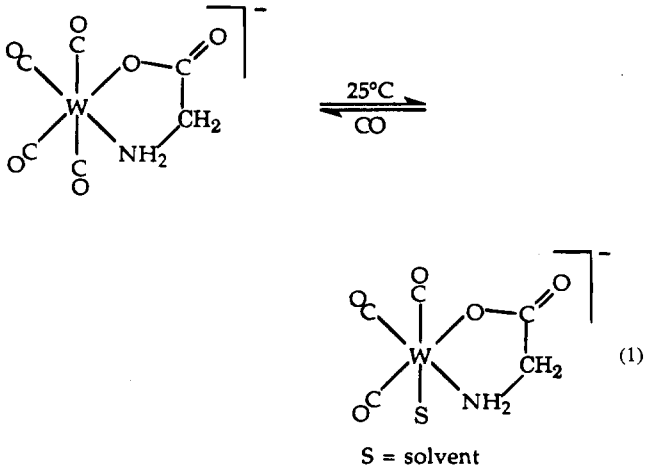

(1)

As indicated in eq 1 the reaction is readily reversible, for there is a rapid and quantitative return of the tricarbonyl derivative to the tetracarbonyl complex (**1**) upon addition of a CO atmosphere, as evidenced by ν(CO) infrared spectroscopy.

Table 10. Atomic Coordinates ($\times 10^4$) and Equivalent Isotropic Displacement Parameters ($Å^2 \times 10^3$) for $[Et_4N][W(CO)_4(O_2CCH_2NMe_2)]$ (**3**)[a]

	x	y	y	U(eq)[b]
W1	1677(1)	2612(1)	3999(1)	30(1)
W2	−1678(1)	7611(1)	1001(1)	30(1)
O1	−319(8)	877(7)	4186(7)	54(6)
O2	2631(10)	534(8)	2948(8)	77(9)
O3	3207(9)	1560(8)	5609(7)	59(6)
O4	296(9)	3820(7)	5424(6)	55(6)
O5	3194(8)	6558(8)	−605(6)	58(6)
O6	−304(9)	8826(7)	−438(6)	55(7)
O7	324(8)	5879(8)	819(7)	57(6)
O8	−2656(9)	5533(8)	2037(7)	68(7)
O9	2993(7)	3888(6)	3760(5)	37(5)
O10	3318(9)	5600(7)	3198(7)	61(7)
O11	−2988(7)	8885(6)	1248(5)	37(5)
O12	−3341(9)	10594(7)	1791(6)	55(7)
N1	900(9)	3688(8)	2797(6)	36(5)
N2	−899(9)	8694(8)	2195(7)	39(6)
N3	6274(9)	2856(8)	4032(7)	42(5)
N4	3737(9)	7847(8)	965(7)	42(6)
C1	441(1)	1521(9)	4101(9)	39(7)
C2	2329(11)	1355(11)	3277(9)	44(7)
C3	2581(9)	1947(10)	4977(8)	36(6)
C4	835(10)	3503(9)	4872(8)	35(7)
C5	−2610(9)	6934(9)	0(8)	32(5)
C6	−840(10)	8483(9)	117(8)	33(7)
C7	−414(11)	6526(10)	892(8)	39(7)
C8	−2335(12)	6367(10)	1713(10)	49(9)
C9	2648(11)	4782(10)	3287(8)	41(6)
C10	1384(12)	4842(10)	2951(9)	48(7)
C11	1247(14)	3254(13)	1950(10)	63(11)
C12	−393(11)	3767(13)	2702(10)	56(7)
C13	−2667(12)	9792(10)	1696(8)	41(7)
C14	−1389(10)	9845(9)	2050(8)	39(6)
C15	−1228(14)	8249(13)	3062(9)	60(11)
C16	374(11)	8763(13)	2283(10)	58(8)
C17	4056(12)	9007(10)	592(9)	47(8)
C18	3250(20)	9962(14)	803(13)	96(17)
C19	2514(12)	7462(14)	542(10)	61(8)
C20	2448(15)	7177(16)	−440(11)	81(11)
C21	4689(11)	7043(9)	732(9)	43(7)
C22	4561(16)	5826(11)	1081(12)	75(13)
C23	3684(10)	7902(10)	1961(8)	36(6)
C24	4790(12)	8248(11)	2507(9)	50(9)
C25	5934(13)	4013(10)	4415(9)	49(8)
C26	6727(19)	4988(13)	4197(12)	90(16)
C27	7487(13)	2446(15)	4461(10)	63(8)
C28	7575(15)	2185(16)	5452(11)	81(11)
C29	5311(10)	2043(9)	4246(9)	41(6)
C30	5435(16)	830(12)	3926(13)	79(13)
C31	6335(10)	2906(10)	3042(8)	39(6)
C32	5220(12)	3267(11)	2503(9)	47(8)

[a] Estimated standard deviations are given in parentheses. [b] Equivalent isotropic U defined as one-third of the trace of the orthogonalized U_{ij} tensor.

Indeed complex **1** undergoes a clean ligand exchange process with ^{13}C-labeled carbon monoxide in CH_3CN to afford ^{13}C-enriched derivatives. The kinetics of ^{13}CO incorporation into complex **1** was monitored by infrared spectroscopy by observing the decrease in the absorbance of the band at 1996 cm^{-1} due to the all ^{12}CO species as a function of time (Figure 5). The rate of the exchange reaction was found to be first order in [**1**] and zero order in [^{13}CO], when carried out in a large excess of ^{13}C-labeled carbon monoxide. The first-order rate constant for CO loss in complex **1** in acetonitrile at 40 °C was determined to be 1.43×10^{-3} s^{-1}. Complex **2** similarly underwent an analogous CO exchange process with a slightly smaller rate constant of 3.37×10^{-4} s^{-1} at 40 °C (Figure 5). On the other hand, complex **3**, which has no N−H linkage, showed no measurable ^{13}CO exchange at 40 °C over a 2-h period. That is, whereas

Table 11. Selected Bond Lengths (Å) and Angles (deg) for $[Et_4N][W(CO)_4(O_2CCH_2NMe_2)]$ (**3**)[a]

W1–C3	1.883(12)	W1–C1	1.933(11)
W1–C4	2.015(12)	W1–C2	2.027(13)
W1–O9	2.188(8)	W1–N1	2.310(10)
W2–C5	1.915(11)	W2–C7	1.965(12)
W2–C8	2.005(12)	W2–C6	2.008(12)
W2–O11	2.193(8)	W2–N2	2.301(10)
O1–C1	1.174(14)	O2–C2	1.156(15)
O3–C3	1.221(14)	O4–C4	1.157(14)
O5–C5	1.160(13)	O6–C6	1.166(14)
O7–C7	1.159(14)	O8–C8	1.169(14)
O9–C9	1.307(14)	O10–C9	1.246(15)
O11–C13	1.290(14)	O12–C13	1.243(15)
N1–C10	1.469(15)	N1–C11	1.471(16)
N1–C12	1.492(15)	N2–C14	1.472(15)
N2–C16	1.469(16)	N2–C15	1.493(15)
C14–C13	1.519(17)	C9–C10	1.498(18)
C3–W1–C1	91.0(5)	C3–W1–C4	88.5(5)
C1–W1–C4	82.8(5)	C3–W1–C2	84.8(5)
C1–W1–C2	83.5(5)	C4–W1–C2	164.6(5)
C3–W1–O9	94.2(4)	C1–W1–O9	174.6(4)
C4–W1–O9	98.6(4)	C2–W1–O9	95.7(4)
C3–W1–N1	167.8(4)	C1–W1–N1	101.2(5)
C4–W1–N1	93.0(4)	C2–W1–N1	96.5(5)
O9–W1–N1	73.6(3)	C5–W2–C7	91.6(5)
C5–W2–C8	84.8(5)	C7–W2–C8	84.4(5)
C5–W2–C6	87.6(5)	C7–W2–C6	81.6(5)
C8–W2–C6	163.9(5)	C5–W2–O11	94.2(4)
C7–W2–O11	174.2(4)	C8–W2–O11	95.4(4)
C6–W2–O11	99.2(4)	C5–W2–N2	167.4(4)
C7–W2–N2	101.0(5)	C8–W2–N2	96.9(5)
C6–W2–N2	93.7(4)	O11–W2–N2	73.2(3)
C9–O9–W1	117.3(8)	C13–O11–W2	119.0(8)
C10–N1–C11	108.6(10)	C10–N1–C12	108.4(10)
C11–N1–C12	107.8(11)	C10–N1–W1	105.6(7)
C11–N1–W1	111.8(8)	C12–N1–W1	114.4(8)
C14–N2–C16	109.5(10)	C14–N2–C15	108.6(10)
C16–N2–C15	106.7(11)	C14–N2–W2	106.0(7)
C16–N2–W2	113.7(8)	C15–N2–W2	112.2(8)
O1–C1–W1	177.9(11)	O2–C2–W1	170.2(12)
O3–C3–W1	176.7(10)	O4–C4–W1	167.5(9)
O5–C5–W2	177.7(10)	O6–C6–W2	169.5(9)
O7–C7–W2	179.2(12)	O8–C8–W2	169.9(13)
O10–C9–O9	121.1(12)	O10–C9–C10	121.4(11)
O9–C9–C10	117.1(11)	N1–C10–C9	110.4(10)
O12–C13–O11	122.3(12)	O12–C13–C14	122.2(11)
O11–C13–C14	115.4(10)	N2–C14–C13	111.3(9)

[a] Estimated standard deviations are given in parentheses.

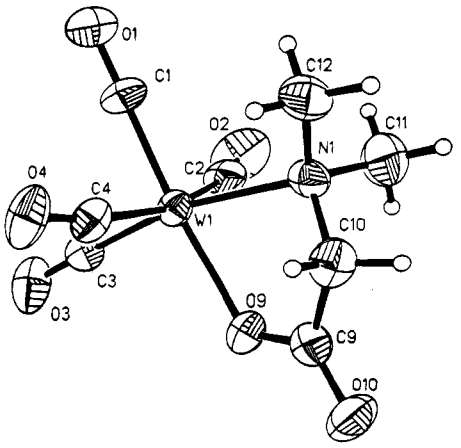

Figure 4. ORTEP diagram of one of the independent anions of complex **3**, showing 50% probability thermal motion ellipsoids with atomic numbering scheme.

the glycine and *N*-methylglycine complexes have quite labile CO ligands, the *N,N*-dimethylglycine derivative does not undergo CO loss under identical conditions.

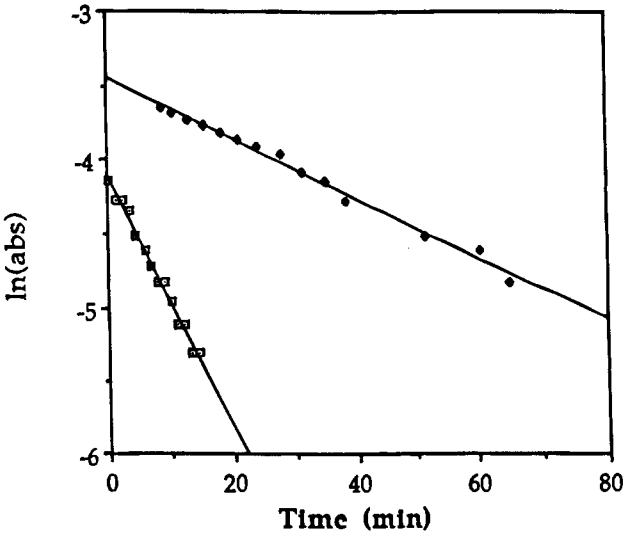

Figure 5. Comparative kinetic data for ^{13}CO exchange in complex **1** (□) and complex **2** (♦) in acetonitrile at 40 °C.

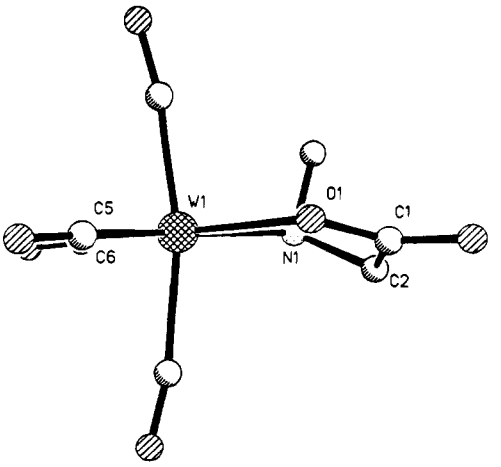

Figure 6. Ball and stick representation of the anion of complex **2** illustrating the puckered five-membered glycinate chelate ring.

Discussion

The coordination environments about the tungsten centers of the three glycine derivatives reported herein are essentially the same. That is, the geometry of the anion is that of a slightly distorted octahedral arrangement of four carbonyl ligands and a puckered five-membered glycinate chelate ring (Figure 6). The plane containing the tungsten center with two equatorial carbon monoxide ligands, along with the N and O atoms of the glycinate ligand, has mean deviations of 0.1045, 0.0264, and 0.0120 Å for complexes **1**–**3**, respectively. A representative description of the structural parameters for the glycinate ring geometry about the metal center with its concomitant effect on the two equatorial CO groups is depicted in Figure 7 for the *N,N*-dimethylglycine derivative. It is noteworthy for the reactivity studies that the W–C bond distances are quite normal for anionic tungsten(0) carbonyls. Furthermore, the CO ligands mutually *trans* to one another (i.e., the axial CO ligands) display W–C bond lengths significantly longer than the corresponding distances for the two equatorial CO ligands; e.g., in **2** these are 2.025[7] *vs* 1.976(9) and 1.947(8) Å, respectively. The electronic similarities of the three anions in solution are quite obvious as well, as revealed by infrared and ^{13}C NMR spectroscopies.

Hence, the only significant structural difference among complexes **1**–**3** in the solid state is the lack of an extended

Scheme 3

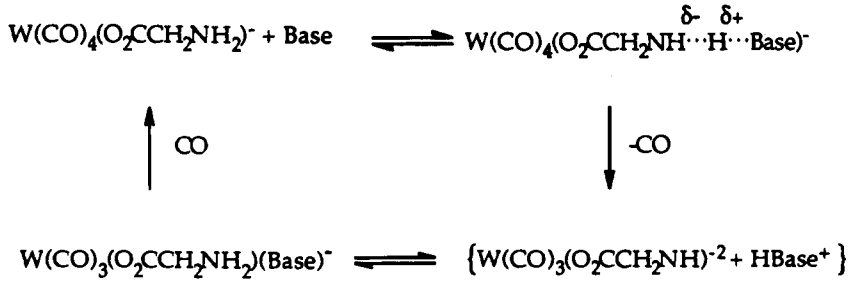

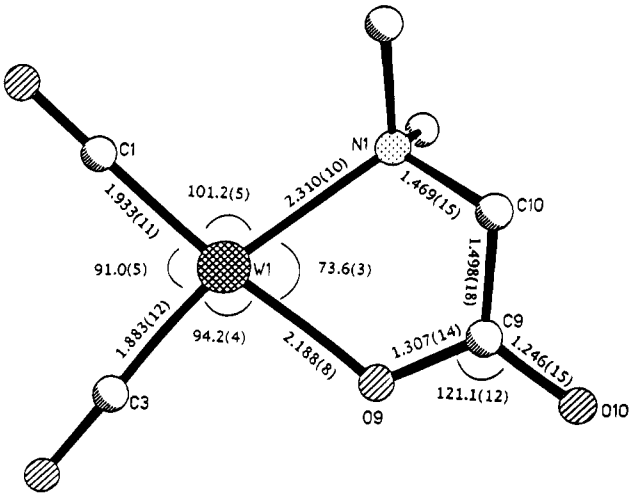

Figure 7. Typical bond lengths and bond angles in the $W(CO)_4$-(glycinate)$^-$ derivatives, as found in complex **3**.

hydrogen-bonding network in the *N,N*-dimethylglycine derivative. Additionally, on the basis of infrared spectroscopy, hydrogen bonding between the amino functionality and the solvent exists in acetonitrile or THF solutions, albeit weaker than that seen between the tungsten anions in the solid state. Indeed, it is this hydrogen bonding observed in complexes **1** and **2**, and not possible in **3**, which we ascribe to the greatly enhanced CO lability noted in the anions of **1** and **2** (eq 2).

$$W(CO)_4(O_2CCH_2NHR)^- + {}^{13}CO \rightleftharpoons W({}^{13}CO)_4(O_2CCHNHR)^- + {}^{12}CO \quad (2)$$

$$R = H, Me$$

Specifically, we attribute the enhanced CO lability noted in complexes **1** and **2**, and not in **3**, to a base- (solvent-) assisted removal of a proton from the amine ligand leading to a substitutionally labile amide complex (Scheme 3). This is analogous to the well-studied conjugate base mechanism of metal amine complexes.[17-22] Deprotonation of the amine ligand is greatly aided by the π-donation of the thus procreated amide ligand to the coordinatively unsaturated metal center in the intermediate species, which is shown in braces in Scheme 3.[23,24] Consistent with this scheme, the $-NH_2$ linkage was observed to undergo facile exchange with D_2O in acetonitrile. In addition, in a closely related system under study in our laboratories, $W(CO)_4(OC_6H_4NH_2)^-$ was found to react with strong base to provide the coordinatively unsaturated $W(CO)_3(OC_6H_4NH)^{2-}$ derivative stabilized by the π-bonding amide and aryloxide ligands. This process corresponds to $W(CO)_4(catecholate)^{2-}$ rapidly undergoing CO substitution *via* the structurally characterized $W(CO)_3(catecholate)^{2-}$ intermediate.[25] Indeed, several unsolvated, coordinatively unsaturated tricarbonyl group 6 metal anions stabilized by π-donor ligands have been characterized by X-ray crystallography.[25-28]

More intimate mechanistic aspects of the ^{13}CO exchange reaction described in eq 2 were examined *via* ^{13}C NMR spectroscopy. A sample of complex **1** was prepared in acetonitrile-d_3 and maintained at −78 °C under an atmosphere of ^{13}CO and placed in a cooled NMR probe. Spectra were collected while the probe temperature was slowly raised until the CO exchange process could be observed (approximately 15 °C). The intensity of all the carbonyl resonances increased simultaneously, maintaining the 2:1:1 ratio for the axial and equatorial carbonyl ligands. Hence, either there is no selectivity for CO exchange or the barrier for intramolecular scrambling in the five-coordinate intermediate is similar to or less than that for intermolecular ligand substitution. Moreover, this same experiment was carried out at 700 psi of $^{13}CO/^{12}CO$ by *in situ* high-pressure NMR with no indication of $W(CO)_5(O_2CCH_2NH_2)^-$ formation, hence ruling out the alternative mechanism for ^{13}CO exchange involving rapid CO addition to **1** followed by CO dissociation. Indeed, the rate of CO exchange is much faster than that expected for CO loss in either tungsten pentacarbonyl isomer.

Acknowledgment. The financial support of this research by the National Science Foundation (Grant CHE91-19737) is greatly appreciated.

Supplementary Material Available: Tables of anisotropic thermal parameters and H atom coordinates for complexes **1**−**3** (8 pages). Ordering information is given on any current masthead page.

(17) Tobe, M. L. *Adv. Inorg. Bioinorg. Mech.* **1983**, *2*, 1.
(18) Garrick, F. J. *Nature (London)* **1937**, *139*, 507.
(19) Dixon, N. E.; Jackson, W. G.; Marty, W.; Sargeson, A. M. *Inorg. Chem.* **1982**, *21*, 688.
(20) Gaudin, M. J.; Clark, C. R.; Buckingham, D. A. *Inorg. Chem.* **1986**, *25*, 2569.
(21) Buckingham, D. A.; Marzilli, P. A.; Sargeson, A. M. *Inorg. Chem.* **1969**, *8*, 1595.
(22) Watson, A. A.; Prinsep, M. R.; House, D.A. *Inorg. Chim. Acta* **1986**, *115*, 95.
(23) Poulton, J. T.; Folting, K.; Streib, W. E.; Caulton, K. G. *Inorg. Chem.* **1992**, *31*, 3191.
(24) Poulton, J. T.; Sigalas, M. P.; Folting, K.; Streib, W. E.; Eisenstein, O.; Caulton, K.G. *Inorg. Chem.* **1994**, *33*, 1476.
(25) Darensbourg, D. J.; Klausmeyer, K. K.; Mueller, B. L.; Reibenspies, J. H. *Angew. Chem. Int. Ed. Engl.* **1992**, *31*, 1503.
(26) Sellmann, D.; Ludwig, W.; Huttner, G.; Zsolnai, L. *J. Organomet. Chem.* **1985**, *294*, 199.
(27) Ashby, M. T.; Enemark, J. H. *J. Am. Chem. Soc.* **1986**, *108*, 730.
(28) Sellmann, D.; Wilke, M.; Knoch, F. *Inorg. Chem.* **1993**, *32*, 2534.